Transition to high-dimensional chaos in nonsmooth dynamical systems

Ru-Hai Du,[1] Shi-Xian Qu,[1,*] and Ying-Cheng Lai[1,2,3]

[1]*School of Physics and Information Technology, Shaanxi Normal University, Xi'an 710062, China*

[2]*School of Electrical, Computer and Energy Engineering, Arizona State University, Tempe, Arizona 85287, USA*

[3]*Department of Physics, Arizona State University, Tempe, Arizona 85287, USA*

(Received 24 June 2018; published 13 November 2018)

We uncover a route from low-dimensional to high-dimensional chaos in nonsmooth dynamical systems as a bifurcation parameter is continuously varied. The striking feature is the existence of a finite parameter interval of periodic attractors in between the regimes of low- and high-dimensional chaos. That is, the emergence of high-dimensional chaos is preceded by the system's settling into a totally nonchaotic regime. This is characteristically distinct from the situation in smooth dynamical systems where high-dimensional chaos emerges directly and smoothly from low-dimensional chaos. We carry out an analysis to elucidate the underlying mechanism for the abrupt emergence and disappearance of the periodic attractors and provide strong numerical support for the typicality of the transition route in the pertinent two-dimensional parameter space. In view of the previous understanding that chaos is typically robust (i.e., without periodic windows) in nonsmooth dynamical systems, the occurrence of a parameter regime of periodic attractors between low- and high-dimensional chaos is unexpected. The finding has implications to applications where high-dimensional and robust chaos is desired.

DOI: 10.1103/PhysRevE.98.052212

I. INTRODUCTION

In nonlinear dynamical systems, there are two kinds of chaos: low dimensional and high dimensional. The characteristic feature of a low-dimensional chaotic invariant set (e.g., an attractor) is that it has only one positive Lyapunov exponent, examples of which include the classic Lorenz [1] and Rössler [2] attractors. High-dimensional chaotic sets are those that possess more than one positive Lyapunov exponent [3–6]. The difference between low- and high-dimensional chaos can be appreciated in terms of significant issues such as control. The well established Ott-Grebogi-Yorke paradigm [7,8] of controlling chaos is most effective for low-dimensional chaotic systems, and controlling high-dimensional chaos [8–10] has remained to be a challenging problem.

In nonlinear dynamics, the four routes to chaos, namely, period-doubling [11], intermittency [12], crisis [13], and quasiperiodicity [14–16], concerned the bifurcation to a low-dimensional chaotic attractor. There was also work on the transition from low- to high-dimensional chaos [17–21] in smooth dynamical systems. A general phenomenon is that the second Lyapunov exponent passes through zero and becomes positive smoothly as a parameter changes through the transition point. Heuristically, this can be understood in light of transition to chaos in random dynamical systems [22–26], in systems with a symmetry [27], and in quasiperiodically driven systems [28–30]. In particular, before the transition, the system is already chaotic with one positive Lyapunov exponent—the largest exponent giving the exponential growth of an infinitesimal vector in the corresponding tangent subspace. For convenience, we call it the primary tangent subspace. The evolution of the vector in the secondary tangent subspace corresponding to the second nontrivial Lyapunov exponent can then be regarded as being subject to an indirect, chaotic or effectively "random" driving from the dynamics in the primary tangent subspace. Under such a driving, an infinitesimal vector in the secondary tangent subspace will exhibit temporal episodes of "expansion" or "contraction," a generic feature in random dynamical systems [22]. The second nontrivial Lyapunov exponent will then exhibit fluctuations in finite time between positive and negative values. The asymptotic value of the exponent depends on the relative weights of the underlying infinitesimal tangent vector in the expanding or contracting phase [17]: the value is negative if the contraction phase over weighs the expansion phase, and vice versa for a positive value. Transition to high-dimensional chaos occurs when the contraction and expansion weights are balanced. Since the weights vary smoothly with the bifurcation parameter [17], the second nontrivial Lyapunov exponent passes through zero smoothly. The generic feature associated with the transition in smooth dynamical systems is thus that high-dimensional chaos arises directly and smoothly from low-dimensional chaos [17–19].

In this paper, we investigate the transition to high-dimensional chaos in nonsmooth dynamical systems that arise commonly in physical, engineering, and biological applications such as impact oscillators [31–36], electronic circuits [37–39], and neuronal networks [40,41]. Mathematically, a typical representation of such systems is piecewise smooth systems, e.g., a one-dimensional piecewise smooth map that can generate low-dimensional chaos. For a system with two pieces, the phase space can be divided into two regions where the dynamical equations in each region are different but are nevertheless smooth, with a border separating the two regions. This setting is representative of physical

*Corresponding author. sxqu@snnu.edu.cn

 ©2018 American Physical Society

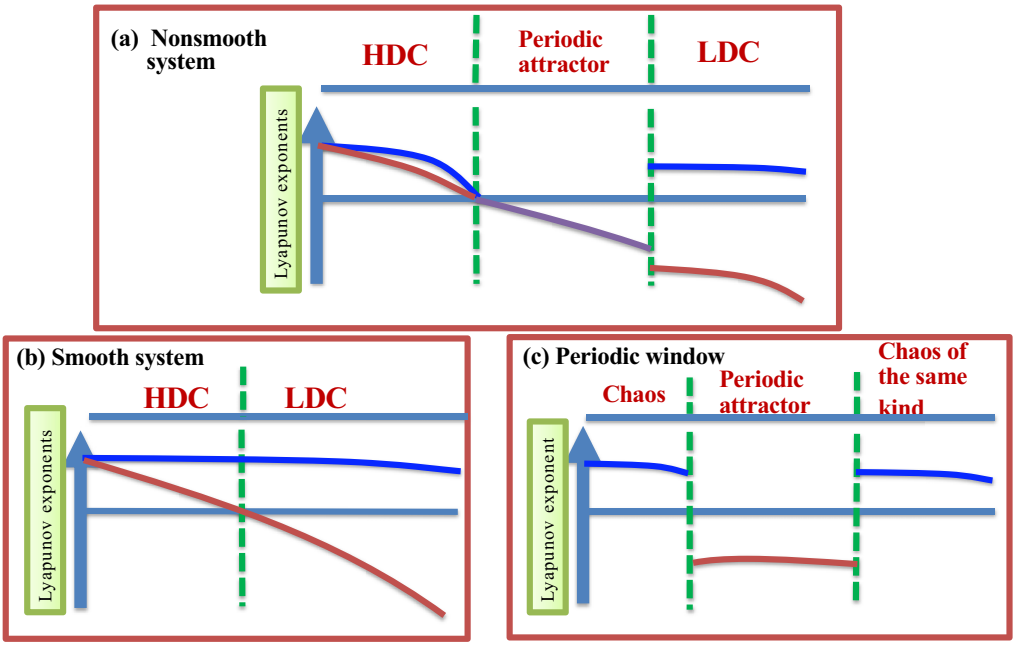

FIG. 1. Schematic illustration of transition scenarios to high-dimensional chaos (HDC) in nonsmooth and smooth dynamical systems. (a) The main result of the paper. As a parameter (e.g., the coupling strength) is reduced from the regime of low-dimensional chaos (LDC) with a single positive Lyapunov exponent, an open parameter interval of periodic attractors arises before HDC emerges. This transition scenario should be contrasted to that in smooth dynamical systems in (b) and is also fundamentally different from the dynamical behavior before and after the occurrence of a periodic window in (c). (b) Transition to HDC in smooth dynamical systems where the second largest Lyapunov exponent passes through zero smoothly at the transition point. That is, HDC emerges exactly where LDC ends. (c) The behavior about a periodic window, where chaos on both sides of the window is of the same kind: either low dimensional or high dimensional.

systems such as electronic switching circuits [37–39]. Previous mathematical analyses of piecewise smooth systems with low-dimensional chaos revealed interesting phenomena such as period-adding bifurcations and transition to chaos from a periodic attractor of arbitrary period, as a result of "border collision" in phase space [42–49]. Because our goal is to uncover and understand how high-dimensional chaos may arise from low-dimensional chaos in nonsmooth systems, we consider the minimal setting of two coupled piecewise smooth subsystems, each capable of exhibiting low-dimensional chaos. At zero coupling, the two subsystems are isolated and the system as a whole has two positive Lyapunov exponents—a trivial type of high-dimensional chaos. In the weak coupling regime, there is interaction between the two subsystems and the system possesses high-dimensional chaos. In the strong coupling regime, synchronization between the two subsystems can occur, and the dynamics of the full system are effectively those of a single subsystem. As a result, the system exhibits low-dimensional chaos. In the intermediate coupling regime, a transition between low- and high-dimensional chaos can be expected. Is the transition scenario any different than that in smooth dynamical systems?

The main finding of this paper is that, in nonsmooth dynamical systems, there can be two distinct routes to high-dimensional chaos: one that is similar to and another characteristically different from that in smooth dynamical systems. In particular, depending on the system parameter values, high-dimensional chaos can arise directly and smoothly from low-dimensional chaos, as in smooth dynamical systems. The striking phenomenon is the existence of an open parameter region in nonsmooth systems where a nonchaotic, "buffer" regime with a periodic attractor arises in between regions of low- and high-dimensional chaos. For example, for the minimal coupled nonsmooth system, as the coupling parameter is decreased from the low-dimensional, synchronous chaos regime, a periodic attractor can arise abruptly and last for a finite parameter interval. At a smaller parameter value, a high-dimensional chaotic attractor emerges abruptly from the periodic attractor. The "buffer" periodic attractor occurs in an open interval of the coupling parameter. In a two-dimensional parameter space, the buffer or "precursor" periodic attractor occupies a finite region—a "bubble," signifying its typicality. The emergence of the bubble region can generally be attributed to border collision bifurcations, for which we provide a detailed analysis. The same transition scenario can occur when the phase space dimension is much larger than 2, e.g., in a system of a large number of coupled nonsmooth maps. In such a case, high-dimensional chaos manifests itself as synchronous clusters with distinct chaotic behaviors, low-dimensional chaos corresponds to globally synchronous chaos, and periodic synchronization occurs in the bubble region. A schematic illustration of our main result and its characteristic difference from the transition scenario in smooth dynamical systems as well as from that around a periodic window is presented in Fig. 1.

We remark on the broad relevance of our work. Uncovering the transition routes to chaos has been a fundamental issue in nonlinear dynamics, but the well documented routes mostly concern the emergence of chaos, low-dimensional [11–16,50] or high-dimensional [17–21], in smooth dynamical systems.

For nonsmooth dynamical systems, the issue of transition to chaos was relatively less studied, with border-collision bifurcation [42–49] as the only known route to low-dimensional chaos. The finding of this paper represents a useful contribution to the fundamentals of nonsmooth dynamical systems that occur in physics, engineering, and biology in contexts such as impact oscillators [31–36], electronic circuits [37–39], and neuronal networks [40,41].

II. MODEL AND RESULTS

A. A system of coupled piecewise linear maps and Lyapunov exponents

A typical class of nonsmooth dynamical systems is piecewise smooth maps [51–55]. To investigate the transition route to high-dimensional chaos, we use coupled map lattices [56–65]. Specifically, we consider the following system of N globally coupled, piecewise smooth maps:

$$x_{n+1}(i) = (1-\varepsilon) f[x_n(i)] + \frac{\varepsilon}{N}\sum_{j=1}^{N} f[x_n(j)], \tag{1}$$

where $x_n(i)$ is the dynamical variable of the ith node at time n, $\varepsilon \in [0, 1]$ is a coupling parameter, and $f(x)$ represents the nodal dynamics. To be concrete, we consider the following one-dimensional piecewise linear map:

$$f(x) = \begin{cases} \alpha x - \mu, & x < 0, \\ \beta x - \mu - \gamma, & x > 0, \end{cases} \tag{2}$$

where α, β, μ and γ are parameters. There is a nonsmooth border at $x = 0$ where the left and right limits of the mapping function are not identical. To investigate the transition to high-dimensional chaos, we require that the isolated nodal dynamics generate a low-dimensional chaotic attractor, which can be realized for, e.g., the following parameter setting: $\alpha = 0.4$, $\beta = -8$, $\mu = 0.1$, and $\gamma = 0$. The Lyapunov exponent of this attractor is $\lambda_0 \approx 0.251$.

A typical dynamical state of system (1) is cluster formation, where the dynamics of all nodes within a cluster are synchronized but those among different clusters are unsynchronized. For simplicity, we consider the case of a two-cluster state [63]:

$$\begin{aligned} x_n(1) = x_n(2) = \cdots = x_n(N_1) = x_n, \\ x_n(N_1+1) = x_n(N_1+2) = \cdots = x_n(N) = y_n, \end{aligned} \tag{3}$$

where N_1 and $N_2 = N - N_1$ are the numbers of nodes in the two clusters. Because of synchronization within each cluster, we obtain an effective two-dimensional nonsmooth map:

$$\begin{aligned} x_{n+1} &= [1-\varepsilon(1-r)] f(x_n) + \varepsilon(1-r) f(y_n), \\ y_{n+1} &= \varepsilon r f(x_n) + (1-\varepsilon r) f(y_n), \end{aligned} \tag{4}$$

where $r = N_1/N$ is the fraction of nodes belonging to the x cluster. In the thermodynamic limit $N \to \infty$, r is a continuous parameter. System (4) describes the dynamical evolution of the two cluster state in system (1). For $r = 1/2$, the two clusters are symmetric with respect to each other [63]. As we will demonstrate, the two distinct routes to high-dimensional chaos occur in different intervals of r values.

Because of the mirror symmetry with respect to $r = 1/2$, we introduce the parameter $\bar{r} = r - 1/2$ to rewrite Eq. (4) as

$$\begin{aligned} x_{n+1} &= \left[1 - \varepsilon\left(\tfrac{1}{2} - \bar{r}\right)\right] x_n + \varepsilon\left(\tfrac{1}{2} - \bar{r}\right) y_n, \\ y_{n+1} &= \varepsilon\left(\tfrac{1}{2} + \bar{r}\right) x_n + \left[1 - \varepsilon\left(\tfrac{1}{2} + \bar{r}\right)\right] y_n, \end{aligned} \tag{5}$$

which has an exact synchronous solution: $x_n = y_n = s_n$. We write $\mathbf{x}_{n+1} = \mathbf{F}(\mathbf{x}_n)$, where $\mathbf{x} \equiv (x, y)^T$ and the symbol "T" denotes transpose. The corresponding variational equations are

$$\begin{pmatrix} \delta x_{n+1} \\ \delta y_{n+1} \end{pmatrix} = f'(s_n) \begin{pmatrix} 1 - \varepsilon\left(\frac{1}{2} - \bar{r}\right) & \varepsilon\left(\frac{1}{2} - \bar{r}\right) \\ \varepsilon\left(\frac{1}{2} + \bar{r}\right) & 1 - \varepsilon\left(\frac{1}{2} + \bar{r}\right) \end{pmatrix} \begin{pmatrix} \delta x_n \\ \delta y_n \end{pmatrix}, \tag{6}$$

where $\delta x_n = x_n - s_n$, $\delta y_n = y_n - s_n$, and $f'(s_n)$ is the derivative of the map function evaluated at the synchronization manifold. The two eigenvalues of the coupling matrix are $u_1 = 1$ and $u_2 = 1 - \varepsilon$. The corresponding transform matrix is given by

$$\mathbf{Q} = \begin{pmatrix} 1 & \frac{\bar{r} - \frac{1}{2}}{\frac{1}{2} + \bar{r}} \\ 1 & 1 \end{pmatrix}. \tag{7}$$

The transform $(\delta\tilde{x}_n, \delta\tilde{y}_n)^T = \mathbf{Q}^{-1} \cdot (\delta x_n, \delta y_n)^T$ leads to a diagonally decoupled form of Eq. (6):

$$\begin{pmatrix} \delta\tilde{x}_{n+1} \\ \delta\tilde{y}_{n+1} \end{pmatrix} = f'(s_n) \begin{pmatrix} 1 & 0 \\ 0 & 1 - \varepsilon \end{pmatrix} \begin{pmatrix} \delta\tilde{x}_n \\ \delta\tilde{y}_n \end{pmatrix}. \tag{8}$$

The transverse Lyapunov exponent is given by

$$\lambda_\perp = \ln(1-\varepsilon) + \lambda_0, \tag{9}$$

where $\lambda_0 > 0$ is the Lyapunov exponent of the chaotic attractor of the individual map. Stable synchronization can be achieved for $\lambda_\perp < 0$. The critical value of the coupling parameter above which synchronization occurs is $\varepsilon_c = 1 - e^{-\lambda_0} \approx 0.222$.

The Lyapunov exponents of the asymptotic invariant set of the system can be calculated from the Jacobian matrix $\mathbf{DF}$ associated with a typical trajectory $\{(x_n, y_n)\}_{n=0}^{\infty}$:

$$\mathbf{DF}^n(x_0, y_0) = \prod_{j=0}^{n-1} \mathbf{DF}(x_j, y_j). \tag{10}$$

The eigenvalues of the Jacobian matrix are given by

$$\det(\mathbf{DF}^n - u\mathbf{I}) = 0. \tag{11}$$

We have that the eigenvalue u satisfies

$$u^2 - \tau u + \Delta = 0, \tag{12}$$

where $\tau \equiv \mathrm{trace}(\mathbf{DF}^n)$ and $\Delta \equiv \det(\mathbf{DF}^n)$. For $\tau^2 - 4\Delta \geqslant 0$, the eigenvalues are real and the Lyapunov exponents are given by

$$\lambda_1 = \frac{1}{n}\ln|u_1|, \quad \lambda_2 = \frac{1}{n}\ln|u_2|, \tag{13}$$

where $u_1 = (\tau + \sqrt{\tau^2 - 4\Delta})/2$ and $u_2 = (\tau - \sqrt{\tau^2 - 4\Delta})/2$. For $\tau^2 - 4\Delta < 0$, we obtain a pair of complex conjugate eigenvalues. In this case, the Lyapunov exponents

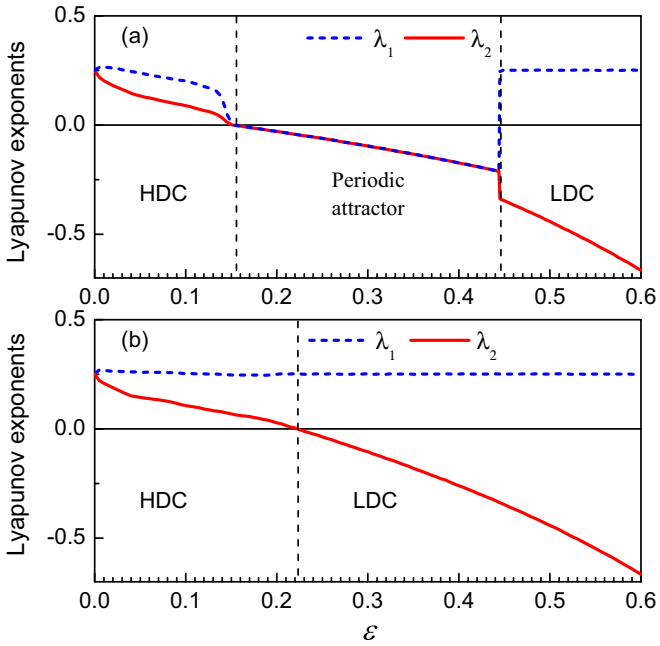

FIG. 2. Two distinct routes of transition to high-dimensional chaos in nonsmooth dynamical systems. (a) For $\bar{r} = 0.3$, the transition route follows the scenario in Fig. 1(a). As the coupling parameter ε is decreased from a relatively large value where there is synchronous chaos with one positive Lyapunov exponent (LDC), a periodic attractor arises. A high-dimensional chaotic attractor with two positive Lyapunov exponents (HDC) emerges when the periodic attractor disappears. (b) For $\bar{r} = 0.48$, HDC arises directly and smoothly from LDC as in smooth dynamical systems.

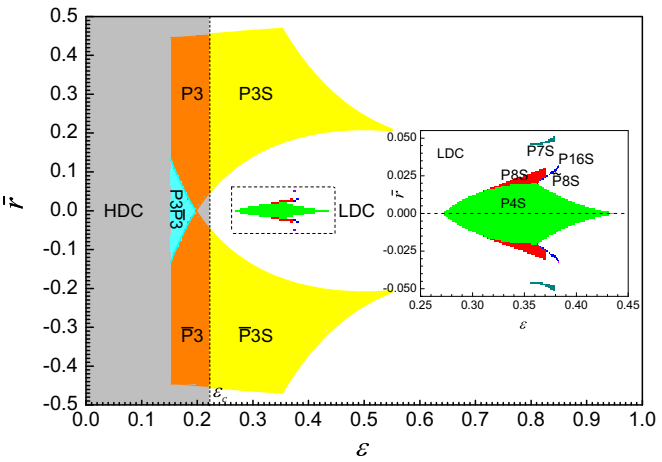

FIG. 3. Phase diagram of distinct attractors in the parameter plane $(\varepsilon, \bar{r})$. There is a mirror symmetry with respect to $\bar{r} = 0$. A period-m attractor is denoted as Pm. The vertical dashed line represents the critical value ε_c of the coupling parameter beyond which synchronous chaos arises. Legends are as follows: HDC, high-dimensional chaos; LDC, low-dimensional chaos (fully synchronous chaotic state, the blank region); P3, clockwise period-3 attractor; P̄3, counterclockwise period-3 attractor. Additional legends are P3P̄3, coexistence of two distinct period-3 attractors; P3S, coexistence of a clockwise period-3 attractor with LDC; P̄3S, counterclockwise period-3 attractor coexisting with LDC. Inset is magnification of the region enclosed by the dashed rectangular box in which periodic attractors of high periods (e.g., P8 and P̄8) coexist with LDC.

are determined by the absolute value of the eigenvalues $|u|$. We have

$$\lambda_{1,2} = \frac{1}{n} \ln |\mathrm{Re}(u)|, \tag{14}$$

where $\mathrm{Re}(u) = \Delta$. For a periodic attractor of period m, we have $n = m$.

B. Main result: Coexistence of distinct transition routes to high-dimensional chaos

For system (5), we uncover a distinct route from low-dimensional to high-dimensional chaos as the coupling parameter ε is reduced. In particular, for relatively large values of ε, there is synchronous chaos and the system has a low-dimensional chaotic attractor with one positive Lyapunov exponent. As ε is decreased, a periodic attractor with two identical negative Lyapunov exponents arises abruptly and lasts for a finite parameter interval. High-dimensional chaos with two positive Lyapunov exponents emerges where the periodic attractor disappears. That is, there exists a "buffer" region of some periodic attractor in between low- and high-dimensional chaos. This transition scenario to high-dimensional chaos, as exemplified by Fig. 2(a) [schematically illustrated in Fig. 1(a)] for $\bar{r} = 0.3$, is unique for nonsmooth dynamical systems. For a different value of parameter $\bar{r}$, the typical route to high-dimensional chaos in smooth dynamical systems [schematically illustrated in Fig. 1(b)] occurs, where a high-dimensional chaotic attractor emerges directly and smoothly from a low-dimensional chaotic attractor, as demonstrated in Fig. 2(b) for $\bar{r} = 0.48$. Nonsmooth dynamical systems thus exhibit richer transition scenarios to high-dimensional chaos than smooth systems.

To obtain a complete picture of the asymptotic attractors in different parameter regions, we calculate the phase diagram in the parameter plane $(\varepsilon, \bar{r})$, as shown in Fig. 3. The phase diagram has a mirror symmetry about $\bar{r} = 0$. For example, the parameter regions in which two distinct period-3 attractors, P3 and P̄3, occur are symmetric about $\bar{r} = 0$. In the strongly coupling regime, synchronous chaotic attractors arise: the system exhibits low-dimensional chaos, whereas high-dimensional chaos occurs in the weakly coupling regime. For $-0.45 \lesssim \bar{r} \lesssim 0.45$, the transition from low- to high-dimensional chaos as the coupling parameter ε is decreased follows the route as demonstrated schematically in Fig. 1(a) and realistically in Fig. 2(a), where the period-3 attractor occupies a large region in the parameter plane. For $0.45 \lesssim |\bar{r}| < 0.5$, the transition from low- to high-dimensional chaos follows the conventional route [Figs. 1(b) and 2(b)] as in smooth dynamical systems. There are also regions in the parameter plane where periodic attractors of various periods arise. For example, the region marked by P3P̄3 is one in which two symmetric period-3 attractors coexist, each with a distinct basin of attraction. There are also periodic attractors as a result of period-doubling bifurcations, such as those denoted as P4, P8, and P16, as well as those created by period-adding bifurcations, e.g., P3, P4, and P7. In the following, we carry out an analysis to elucidate the underlying mechanism for the abrupt emergence

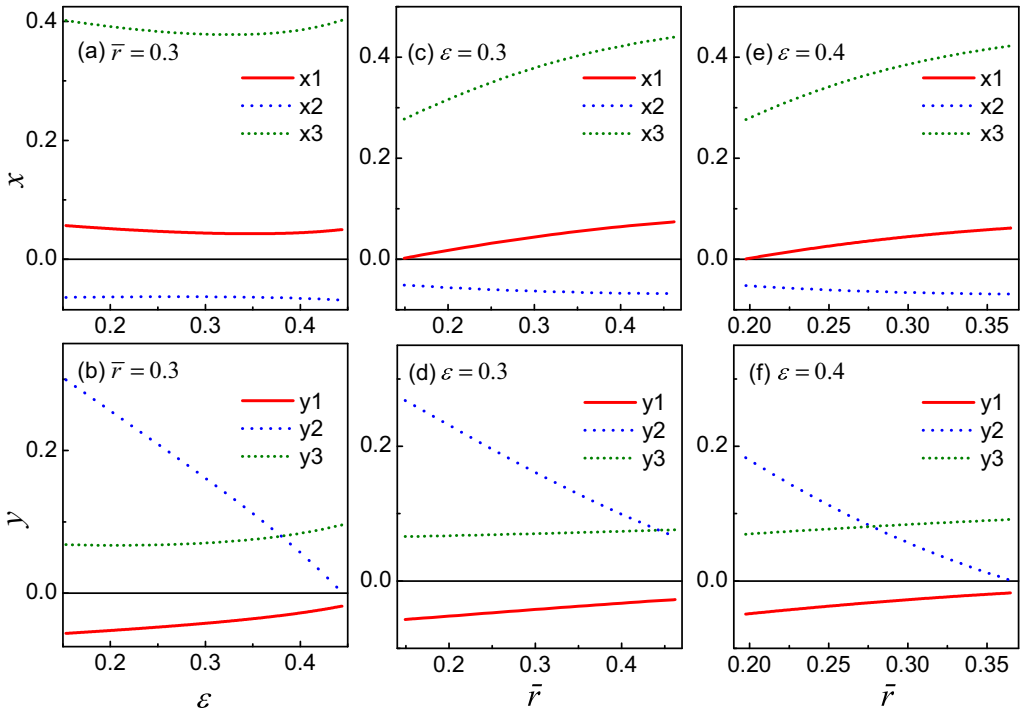

FIG. 4. Emergence and disappearance of a period-3 attractor. The three orbital points are denoted by (x_1^*, y_1^*), (x_2^*, y_2^*), and (x_3^*, y_3^*). Shown are examples of how the orbital points of the period-3 attractor depend on the bifurcation parameter ε or $\bar{r}$: (a),(b) $\bar{r} = 0.3$, (c),(d) $\varepsilon = 0.3$, and (e),(f) $\varepsilon = 0.4$.

of the periodic attractors in between regimes of low- and high-dimensional chaos.

III. EMERGENCE OF PERIODIC ATTRACTORS BETWEEN REGIMES OF LOW- AND HIGH-DIMENSIONAL CHAOS

For nonsmooth dynamical system, linear stability analysis alone is often inadequate to characterize the bifurcations or transitions [63]. We find that, in our piecewise linear systems, the transition from low-dimensional chaos to a periodic attractor is typically of the second order, continuous type. The dynamical origin of the transition is border collision bifurcations.

A. Emergence of period-3 attractors

The period-3 attractors take up a considerable region in the two-dimensional parameter space. In order to determine the stability condition of the attractor, we examine its orbital structure as a bifurcation parameter is continuously varied. Taking advantage of the symmetry of the system, we focus on the region of $\bar{r} \geqslant 0$. The three orbital points are denoted as (x_1^*, y_1^*), (x_2^*, y_2^*), and (x_3^*, y_3^*), where the first point (x_1^*, y_1^*) is located at the bottom of the phase portrait: y_1^* is the minimal value, as shown in Fig. 4. For $\bar{r} = 0.3$, from Figs. 4(a) and 4(b), we see that at the left boundary the stable period-3 attractor disappears without collision, while at the right boundary it disappears because of the collision between the y_2 orbit and the border $y = 0$. The phase space for $\varepsilon = 0.3$ is shown in Figs. 4(c) and 4(d), where the x_1 orbit collides with the border $x = 0$ for a small value of $\bar{r}$ and the stable period-3 attractor disappears without collision for a large value of $\bar{r}$. For $\varepsilon = 0.45$, as shown in Figs. 4(e) and 4(f), we see that the two boundaries of the disappearance of the period-3 attractor are both due to border collision bifurcations. In particular, the x_1 orbit collides with the border $x = 0$ for a small value of $\bar{r}$ and the y_2 orbit collides with the border $y = 0$ for a large value of $\bar{r}$.

Our detailed calculation reveals that there are two types of border collision bifurcations with the critical conditions given by

$$A: \begin{cases} (x_2^*, y_2^*) = \mathbf{F}^3[(x_2^*, y_2^*)], \\ y_2^* = 0^+, \end{cases} \tag{15}$$

$$B: \begin{cases} (x_1^*, y_1^*) = \mathbf{F}^3[(x_1^*, y_1^*)], \\ x_1^* = 0^+, \end{cases} \tag{16}$$

where the superscript "+" denotes the situation where the orbital point collides with the discontinuous border from the positive side. The stability condition of the period-3 attractor can then be obtained. In particular, from Fig. 4, we have that the orbital points of the attractor satisfy the conditions $(x_1^* > 0, y_1^* < 0)$, $(x_2^* < 0, y_2^* > 0)$, and $(x_3^* > 0, y_3^* > 0)$. The Jacobian matrix evaluated at the attractor is

$$\mathbf{DF}^3 = \mathbf{G}\begin{pmatrix} \alpha & 0 \\ 0 & \alpha \end{pmatrix}\mathbf{G}\begin{pmatrix} \beta & 0 \\ 0 & \alpha \end{pmatrix}\mathbf{G}\begin{pmatrix} \alpha & 0 \\ 0 & \beta \end{pmatrix}, \tag{17}$$

with $\mathbf{G}$ being the coupling matrix

$$\begin{pmatrix} 1-\varepsilon\left(\frac{1}{2}-\bar{r}\right) & \varepsilon\left(\frac{1}{2}-\bar{r}\right) \\ \varepsilon\left(\frac{1}{2}+\bar{r}\right) & 1-\varepsilon\left(\frac{1}{2}+\bar{r}\right) \end{pmatrix}. \tag{18}$$

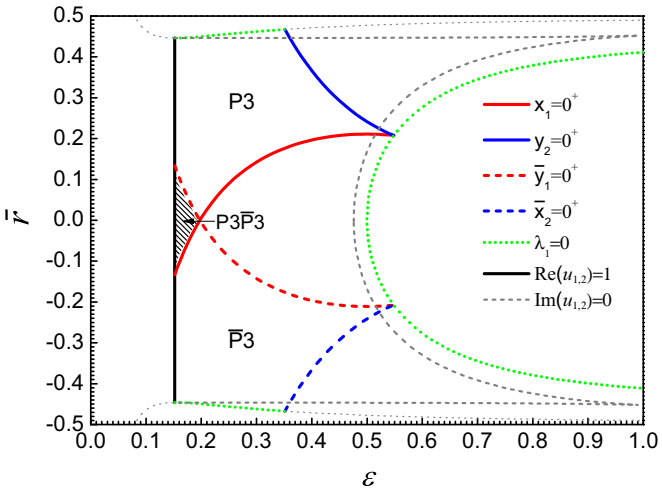

FIG. 5. Analysis of the period-3 attractor. The blue and red curves represent border collision bifurcations. The green dotted curves represent the critical condition for the largest Lyapunov exponent λ_1. The black line denotes the critical condition of the real part of complex conjugate eigenvalues. The dashed lines indicate zero imaginary part of the complex conjugate eigenvalues.

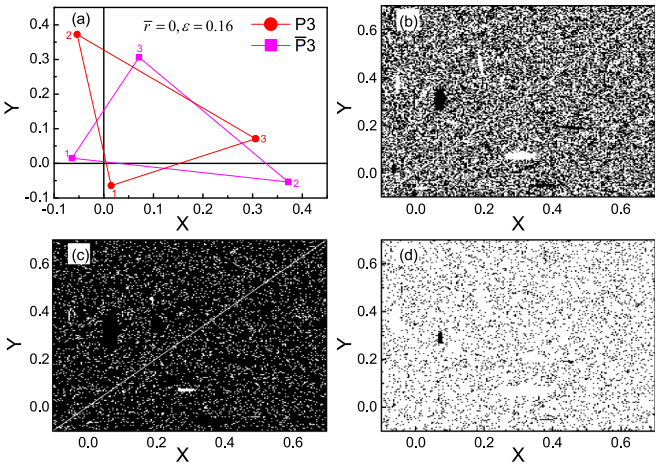

FIG. 6. Coexistence of two distinct period-3 attractors. (a) Two types of period-3 attractors that coexist in phase space. The basins of attraction of the attractors for (b) $\bar{r} = 0$ and $\varepsilon = 0.16$, (c) $\bar{r} = 0.05$ and $\varepsilon = 0.16$, and (d) $\bar{r} = -0.05$ and $\varepsilon = 0.16$, where the dark and blank regions represent the basins of attraction of the P3 and $\bar{\text{P}}3$ attractors, respectively.

From the characteristic equation Eq. (17), we get

$$\Delta = (1-\varepsilon)^3\alpha^4\beta^2,$$
$$\tau = \tfrac{1}{4}\alpha(\varepsilon-2)\{[(4\bar{r}^2-1)(\alpha-\beta)^2 - 4\alpha\beta]\varepsilon^2 - 4\alpha\beta(\varepsilon+1)\}. \quad (19)$$

Combining Eqs. (13)–(16) and (19) leads to the critical conditions for the period-3 attractor to be stable.

Figure 5 shows the results from the stability analysis. The stable period-3 attractor exists in the region surrounded by the curves of stability (denoted by the green dotted curves and the black line) and border collision bifurcations (denoted by red and blue curves). Comparing Fig. 5 with Fig. 3, we find a good agreement between the theoretical analysis and the numerically calculated structure of the parameter space for the period-3 attractor. Specifically, for a fixed value of $\bar{r}$, as the coupling parameter ε is increased, the period-3 attractor undergoes a border collision bifurcation before it becomes unstable, corresponding to the the sudden transition from low-dimensional chaos to a periodic attractor, as shown in Fig. 2. In addition, there is a region surrounded by x_1, $\bar{y}_1$ and the stability curve, as marked by the oblique lines, which explains the emergence of two types of period-3 attractors. Further support for the coexistence of the two types of attractors can be obtained by computing the basins of attraction, as shown in Fig. 6. As the bifurcation parameter is varied, the basins of the two types of period-3 attractors change.

B. Occurrence of periodic attractors of period greater than 3

Combining the linear stability and border collision bifurcation analyses, we can obtain the existing conditions of periodic attractors of various periods. Figure 7 shows the theoretical results for periodic attractors of period 4, 7, 8, and 16 for $\bar{r} \geqslant 0$. We see that, except for the period-4 attractor whose existing condition is determined solely by border collision bifurcation, the emergence and existence of periodic attractors of higher periods are due to the mixed "action" of stability and border collision bifurcation. We also find border collision induced period-doubling bifurcations. For example, a period-8 attractor (P8) arises after the period-4 orbit collides with the discontinuous border, as shown in Fig. 7(c), and a periodic attractor of period 16 emerges after an alternative type of period-8 attractor ($\tilde{\text{P}}8$) collides with the border, as shown in Fig. 7(d). Further, the P8 and $\tilde{\text{P}}8$ attractors can convert into each other through the collision that occurs on the AB curve, as shown in Fig. 7(c). In general, as the period increases, the area of the periodic attractor in the parameter space diminishes quickly.

C. Globally coupled maps

The occurrence of periodic attractors as a precursor of transition to high-dimensional chaos in nonsmooth systems is a general phenomenon that occurs in systems of globally coupled piecewise linear maps [Eq. (1)]. For such a system, a variety of collective dynamical states can arise. In particular, high-dimensional chaos manifests itself as asynchronous chaos, whereas low-dimensional chaos corresponds to globally synchronous chaos and, in the "buffer" region of periodic attractors, periodic synchronization occurs. The parameter region in which various two-cluster states occur is shown in Fig. 8, which qualitatively agrees with the phase diagram in Fig. 3. Note that, not all stable two-cluster states can be observed in a globally coupled system of finite size. In such a system, multistability [66–75] is common, and the basin of attraction of a stable attractor can have a fractal structure, on which small perturbations can have a significant effect. Certain states are thus not physically observable. Note also that the result in Fig. 3 in fact corresponds to the thermodynamic limit $N \to \infty$, but in Fig. 8, the network size N is finite. This leads to the small discrepancies between Figs. 8 and 3.

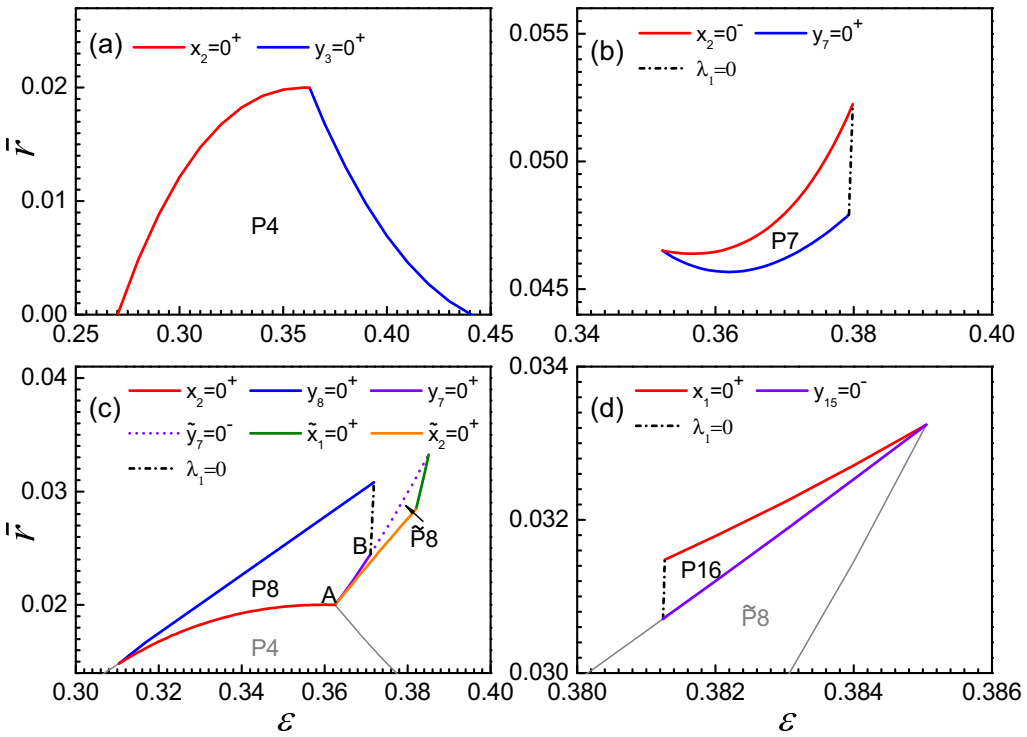

FIG. 7. Rise of periodic attractors of period greater than three. (a)–(d) Theoretically obtained stability regions for period-4, period-7, period-8, and period-16 attractors, respectively.

IV. DISCUSSION

Historically, the discoveries of four distinct routes to low-dimensional chaos with one positive Lyapunov exponent: period-doubling [11], intermittency [12], crisis [13], and quasiperiodicity [14–16], led to fundamental insights into and an understanding of the occurrence of chaotic behaviors in natural systems and henceforth played an important role in the development of nonlinear dynamics. Transition to high-dimensional chaos, chaos with multiple positive Lyapunov exponents, has also been studied but only for smooth dynamical systems [17–21]. In such systems, a typical route to high-dimensional chaos is that the second Lyapunov exponent passes through zero smoothly from the negative side as a system parameter varies. The generality of this route lies in regarding the underlying dynamical system as consisting of a number of mutually interacting subsystems, some exhibiting low-dimensional chaos. The chaotic subsystems then provide a kind of "driving" to other subsystems. As a bifurcation parameter changes, an additional positive Lyapunov exponent can arise. The nature of chaotic driving stipulates that the second exponent becomes positive in a smooth fashion [17–19], a feature that is characteristic of the transition to chaos in random dynamical systems [22–25].

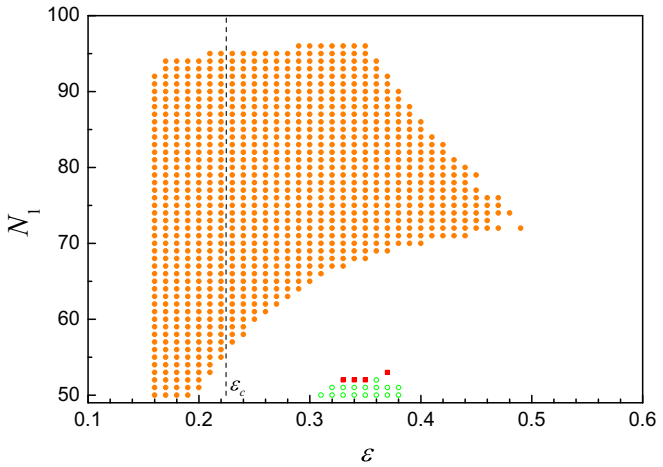

FIG. 8. Two-cluster state in a globally coupled nonsmooth map system. The size of the network is $N = 100$ and N_1 represents the size of the largest cluster. The two-cluster states of period 3, 4, and 8 are represented by the orange solid, green open, and red square dots, respectively. Each state is obtained using 10^5 random initial conditions.

The main question addressed in this paper is whether transition to high-dimensional chaos in nonsmooth dynamical systems can follow a characteristically different route than that in smooth dynamical systems. The answer is affirmative. In particular, using the paradigmatic setting of coupled nonsmooth maps, we have uncovered a route in which a periodic attractor arises as a precursor to high-dimensional chaos. That is, as a bifurcation parameter is varied from the regime of a low-dimensional chaotic attractor, an interval in which the attractor of the system is periodic occurs, after which a high-dimensional chaotic attractor is born. In a two-dimensional parameter space, the regions of low- and high-dimensional chaos are separated by an open, "bubble" region of periodic attractors. As we have shown, the route to high-dimensional chaos is characteristically different from that in smooth dynamical systems, and the associated feature in the parameter space is also distinct from that about the occurrence of a

periodic window (cf., Fig. 1). Our analysis indicates that the emergence of the "bubble" region can be attributed to border collision bifurcations that occur commonly in nonsmooth dynamical systems. Numerical computations have also revealed that there are parameter regions in which a high-dimensional chaotic attractor can arise smoothly from a low-dimensional one, as in smooth dynamical systems. The general finding is then that, in nonsmooth dynamical systems, smooth and discontinuous routes to high-dimensional chaos coexist in the parameter space. From the perspective of transition to high-dimensional chaos, nonsmooth dynamical systems thus offer richer behaviors than smooth dynamical systems.

The finding of this paper has implications to the phenomenon and application of robust chaos [37,76–86], i.e., chaos without periodic windows. In particular, robust chaos is a unique phenomenon in nonsmooth dynamical systems and arises in broad contexts such as electronic circuits [37,77,81–84], neural networks [78], impact oscillators [37], and even electroencephalogram models [79]. In chaos-based applications such as communication [87–93] and inducing chaos in electronic circuits [81–83], robust chaos is desired because the underlying operation depends on the system's being in an uninterrupted chaotic state. It thus seems quite reasonable to exploit nonsmooth dynamical systems for these applications because of the ubiquity of robust chaos in these systems [37,76–86]. Our finding that there are typical situations in nonsmooth dynamical systems where periodic attractors can arise in a parameter interval in between low-dimensional and high-dimensional chaos is thus unexpected. The practical significance is that caution should be exercised when exploiting nonsmooth dynamical systems for robust chaos based applications.

ACKNOWLEDGMENTS

This work was supported by the National Natural Science Foundation of China (Grant No. 11645005). Y.-C.L. would like to acknowledge support from the Vannevar Bush Faculty Fellowship program sponsored by the Basic Research Office of the Assistant Secretary of Defense for Research and Engineering and funded by the Office of Naval Research through Grant No. N00014-16-1-2828.

[1] E. Lorenz, J. Atmos. Sci. **20**, 130 (1963).
[2] O. E. Rössler, Phys. Lett. A **57**, 397 (1976).
[3] K. Ikeda and K. Matsumoto, Physica D **29**, 223 (1987).
[4] E. Barreto, B. R. Hunt, C. Grebogi, and J. A. Yorke, Phys. Rev. Lett. **78**, 4561 (1997).
[5] Z. E. Musielak and D. E. Musielak, Int. J. Bifurcat. Chaos Appl. Sci. Eng. **19**, 2823 (2009).
[6] I. Ispolatov, V. Madhok, S. Allende, and M. Doebeli, Sci. Rep. **5**, 12506 (2015).
[7] E. Ott, C. Grebogi, and J. A. Yorke, Phys. Rev. Lett. **64**, 1196 (1990).
[8] S. Boccaletti, C. Grebogi, Y.-C. Lai, H. Mancini, and D. Maza, Phys. Rep. **329**, 103 (2000).
[9] D. Auerbach, C. Grebogi, E. Ott, and J. A. Yorke, Phys. Rev. Lett. **69**, 3479 (1992).
[10] C. Grebogi and Y.-C. Lai, IEEE Trans. Circ. Syst. **44**, 971 (1997).
[11] M. J. Feigenbaum, J. Stat. Phys. **19**, 25 (1978).
[12] Y. Pomeau and P. Manneville, Commun. Math. Phys. **74**, 189 (1980).
[13] C. Grebogi, E. Ott, and J. A. Yorke, Physica D **7**, 181 (1983).
[14] D. Ruelle and F. Takens, Commun. Math. Phys. **20**, 167 (1971).
[15] J. P. Gollub and H. L. Swinney, Phys. Rev. Lett. **35**, 927 (1975).
[16] S. E. Newhouse, D. Ruelle, and F. Takens, Commun. Math. Phys. **64**, 35 (1978).
[17] M. A. Harrison and Y.-C. Lai, Phys. Rev. E **59**, R3799 (1999).
[18] M. A. Harrison and Y.-C. Lai, Int. J. Bifurcat. Chaos Appl. Sci. Eng. **10**, 1471 (2000).
[19] R. Davidchack and Y.-C. Lai, Phys. Lett. A **270**, 308 (2000).
[20] D. Pazo, E. Sanchez, and M. A. Matias, Int. J. Bifurcat. Chaos **11**, 2683 (2001).
[21] D. Pazo and M. A. Matias, Europhys. Lett. **72**, 176 (2005).
[22] L. Yu, E. Ott, and Q. Chen, Phys. Rev. Lett. **65**, 2935 (1990).
[23] S. Rim, D.-U. Hwang, I. Kim, and C.-M. Kim, Phys. Rev. Lett. **85**, 2304 (2000).
[24] Z. Liu, Y.-C. Lai, L. Billings, and I. B. Schwartz, Phys. Rev. Lett. **88**, 124101 (2002).
[25] Y.-C. Lai, Z. Liu, L. Billings, and I. B. Schwartz, Phys. Rev. E **67**, 026210 (2003).
[26] B. Xu, Y.-C. Lai, L. Zhu, and Y. Do, Phys. Rev. Lett. **90**, 164101 (2003).
[27] Y.-C. Lai, Phys. Rev. E **53**, R4267 (1996).
[28] Y.-C. Lai, Phys. Rev. E **53**, 57 (1996).
[29] Y.-C. Lai, U. Feudel, and C. Grebogi, Phys. Rev. E **54**, 6070 (1996).
[30] T. Yalcinkaya and Y.-C. Lai, Phys. Rev. Lett. **77**, 5039 (1996).
[31] J. M. T. Thompson and R. Ghaffari, Phys. Rev. A **27**, 1741 (1983).
[32] S. W. Shaw and P. J. Holmes, J. Sound. Vib. **90**, 129 (1983).
[33] G. S. Whiston, J. Sound Vib. **118**, 395 (1987).
[34] A. B. Nordmark, J. Sound Vib. **145**, 279 (1991).
[35] W. Chin, E. Ott, H. E. Nusse, and C. Grebogi, Phys. Rev. E **50**, 4427 (1994).
[36] F. Casas, W. Chin, C. Grebogi, and E. Ott, Phys. Rev. E **53**, 134 (1996).
[37] S. Banerjee, J. A. Yorke, and C. Grebogi, Phys. Rev. Lett. **80**, 3049 (1998).
[38] S. Banerjee and C. Grebogi, Phys. Rev. E **59**, 4052 (1999).
[39] S. Banerjee, P. Ranjan, and C. Grebogi, IEEE Trans. Circ. Syst. **47**, 633 (2000).
[40] W. Nicola and S. A. Campbell, SIAM J. Appl. Dyn. Syst. **15**, 391 (2016).
[41] W. Nicola, B. Tripp, and M. Scott, Front. Comput. Neurosci. **10**, 15 (2016).
[42] H. E. Nusse and J. A. Yorke, Physica D **57**, 39 (1992).
[43] H. E. Nusse, E. Ott, and J. A. Yorke, Phys. Rev. E **49**, 1073 (1994).
[44] M. Dutta, H. E. Nusse, E. Ott, J. A. Yorke, and G. Yuan, Phys. Rev. Lett. **83**, 4281 (1999).

[45] J. Lv, T.-S. Zhou, G. R. Chen, and X.-S. Yang, Chaos **12**, 344 (2002).
[46] M. A. Hassouneh, E. H. Abed, and H. E. Nusse, Phys. Rev. Lett. **92**, 070201 (2004).
[47] A. Ganguli and S. Banerjee, Phys. Rev. E **71**, 057202 (2005).
[48] V. Avrutin, M. Schanz, and S. Banerjee, Phys. Rev. E **75**, 066205 (2007).
[49] Y.-H. Do and Y.-C. Lai, Chaos **18**, 043107 (2008).
[50] E. Ott, *Chaos in Dynamical Systems*, 2nd ed. (Cambridge University Press, Cambridge, UK, 2002).
[51] B. Christiansen, D.-R. He, S. Habip, M. Bauer, U. Krueger, and W. Martienssen, Phys. Rev. A **45**, 8450 (1992).
[52] S.-X. Qu, S. Wu, and D.-R. He, Phys. Rev. E **57**, 402 (1998).
[53] J. Wang, X.-L. Ding, B. Hu, B.-H. Wang, J.-S. Mao, and D.-R. He, Phys. Rev. E **64**, 026202 (2001).
[54] Y.-C. Lai, D.-R. He, and Y.-M. Jiang, Phys. Rev. E **72**, 025201 (2005).
[55] K. Yang, X. Wang, and S.-X. Qu, Phys. Rev. E **92**, 022905 (2015).
[56] K. Kaneko, Phys. Rev. Lett. **63**, 219 (1989).
[57] K. Kaneko, Physica D **41**, 137 (1990).
[58] K. Kaneko, Phys. Rev. Lett. **65**, 1391 (1990).
[59] A. Pikovsky, O. Popovych, and Y. Maistrenko, Phys. Rev. Lett. **87**, 044102 (2001).
[60] O. Popovych, Y. Maistrenko, and E. Mosekilde, Phys. Rev. E **64**, 026205 (2001).
[61] O. Popovych, Y. Maistrenko, and E. Mosekilde, Phys. Lett. A **302**, 171 (2002).
[62] A. F. Taylor, P. Kapetanopoulos, B. J. Whitaker, R. Toth, L. Bull, and M. R. Tinsley, Phys. Rev. Lett. **100**, 214101 (2008).
[63] A. Polynikis, M. di Bernardo, and S. J. Hogan, Chaos, Solitons Fractals **41**, 1353 (2009).
[64] A. Pikovsky and M. Rosenblum, Chaos **25**, 097616 (2015).
[65] K. Kaneko, Chaos **25**, 097608 (2015).
[66] U. Feudel, C. Grebogi, B. R. Hunt, and J. A. Yorke, Phys. Rev. E **54**, 71 (1996).
[67] U. Feudel and C. Grebogi, Chaos **7**, 597 (1997).
[68] S. Kraut, U. Feudel, and C. Grebogi, Phys. Rev. E **59**, 5253 (1999).
[69] S. Kraut and U. Feudel, Phys. Rev. E **66**, 015207 (2002).
[70] U. Feudel and C. Grebogi, Phys. Rev. Lett. **91**, 134102 (2003).
[71] C. N. Ngonghala, U. Feudel, and K. Showalter, Phys. Rev. E **83**, 056206 (2011).
[72] M. S. Patel, U. Patel, A. Sen, G. C. Sethia, C. Hens, S. K. Dana, U. Feudel, K. Showalter, C. N. Ngonghala, and R. E. Amritkar, Phys. Rev. E **89**, 022918 (2014).
[73] A. N. Pisarchik and U. Feudel, Phys. Rep. **540**, 167 (2014).
[74] L. Ying, D. Huang, and Y.-C. Lai, Phys. Rev. E **93**, 062204 (2016).
[75] Y.-C. Lai and C. Grebogi, Eur. Phys. J.: Spec. Top. **226**, 1703 (2017).
[76] M. Majumdar and T. Mitra, Ricerche Econ. **48**, 225 (1994).
[77] R. Femat, J. Alvarez-Ramirez, B. Castillo-Toledo, and J. Gonzalez, IEEE Trans. Circ. Syst. **46**, 1150 (1999).
[78] A. Potapov and M. K. Ali, Phys. Lett. A **277**, 310 (2000).
[79] M. P. Dafilis, D. T. J. Liley, and P. J. Cadusch, Chaos **11**, 474 (2001).
[80] P. Kowalczyk, Nonlinearity **18**, 485 (2004).
[81] Y.-C. Lai, A. Kandangath, S. Krishnamoorthy, J. A. Gaudet, and A. P. S. de Moura, Phys. Rev. Lett. **94**, 214101 (2005).
[82] A. Kandangath, S. Krishnamoorthy, Y.-C. Lai, and J. A. Gaudet, IEEE Trans. Circ. Syst. **54**, 1109 (2007).
[83] S. Gopal and Y.-C. Lai, Circ. Syst. Sig. Pr. **28**, 535 (2009).
[84] A. Deshpande, Q. Chen, Y. Wang, Y.-C. Lai, and Y. Do, Phys. Rev. E **82**, 026209 (2010).
[85] P. Glendinning, Eur. Phys. J.: Spec. Top. **226**, 1721 (2017).
[86] E. Zeraoulia and J. C. Sprott, *Robust Chaos and Its Applications*, 1st ed. (World Scientific, Singapore, 2011).
[87] L. M. Pecora and T. L. Carroll, Phys. Rev. Lett. **64**, 821 (1990).
[88] S. Hayes, C. Grebogi, and E. Ott, Phys. Rev. Lett. **70**, 3031 (1993).
[89] K. M. Cuomo and A. V. Oppenheim, Phys. Rev. Lett. **71**, 65 (1993).
[90] E. Bollt, Y.-C. Lai, and C. Grebogi, Phys. Rev. Lett. **79**, 3787 (1997).
[91] J. García-Ojalvo and R. Roy, Phys. Rev. Lett. **86**, 5204 (2001).
[92] V. S. Udaltsov, J.-P. Goedgebuer, L. Larger, and W. T. Rhodes, Phys. Rev. Lett. **86**, 1892 (2001).
[93] H.-P. Ren, M. S. Baptista, and C. Grebogi, Phys. Rev. Lett. **110**, 184101 (2013).